HHS Public Access

Author manuscript

Stroke. Author manuscript; available in PMC 2017 June 01.

Published in final edited form as:

Stroke. 2016 June ; 47(6): 1626–1631. doi:10.1161/STROKEAHA.116.013146.

Hematoma Changes During Clot Resolution After Experimental Intracerebral Hemorrhage

Shenglong Cao, MD[1,2], **Mingzhe Zheng, MD, Ph.D.**[1], **Ya Hua, MD**[1], **Gao Chen, MD, Ph.D.**[2], **Richard F. Keep, Ph.D**[1], and **Guohua Xi, MD**[1]

[1]Department of Neurosurgery, University of Michigan, Ann Arbor, MI, USA

[2]Department of Neurosurgery, the 2nd Affiliated Hospital, Zhejiang University, Hangzhou, China

Abstract

Background and Purpose—Hematoma clearance occurs in the days after intracerebral hemorrhage (ICH) and has not been well studied. In the current study, we examined changes in the hematoma in a piglet ICH model. The effect of deferoxamine on hematoma was also examined.

Methods—The ICH model was induced by an injection of autologous blood into the right frontal lobe of piglets. First, a natural time course of hematoma changes up to 7 days was determined. Second, the effect of deferoxamine on hematoma changes was examined. Hemoglobin and membrane attack complex levels in the hematoma were examined by enzyme-linked immunosorbent assay. Immunohistochemistry and Western blotting was used to examine CD47 (a regulator of erythrophagocytosis), CD163 (a hemoglobin scavenger receptor) and heme oxygenase-1 (a heme degradation enzyme) in the clot.

Results—After ICH, there was a reduction in red blood cell diameter within the clot with time. This was accompanied by membrane attack complex accumulation and decreased hemoglobin levels. Erythrophagocytosis occurred in the hematoma and this was associated with reduced clot CD47 levels. Activated macrophages/microglia were CD163 and hemeoxygenase-1 positive and these accumulated in the clot with time. Deferoxamine treatment attenuated the process of hematoma resolution by reducing member attack complex formation and inhibiting CD47 loss in the clot.

Conclusion—These results indicate that membrane attack complex and erythrophagocytosis contribute to hematoma clearance after ICH, which can be altered by deferoxamine treatment.

Keywords

cerebral hemorrhage; deferoxamine; erythrophagocytosis; hemotoma resolution hemolysis; swine

Correspondence: Guohua Xi, M.D., R5018 BSRB, University of Michigan109 Zina Pitcher Place, Ann Arbor, Michigan 48109-2200, USA, Telephone: (734) 764-1207, guohuaxi@umich.edu.

Potential Conflicts of Interest: We declare that we have no conflict of interest.

Introduction

Hematoma resolution occurs in the days after intracerebral hemorrhage (ICH). The hematoma clearance may be via red blood cell (RBC) lysis or phagocytosis. Erythrocytes within the clot preserve a normal biconcave configuration for a while and then start to lyse. At the same time, erythrocytes are phagocytized by microglia/macrophages.

Erythrocyte lysis after ICH releases hemoglobin and it's degradation products, such as iron, contributing to oxidative stress, delayed brain edema and neuronal death [1]. Erythrocyte lysis after ICH can be mediated by the complement activation and formation of the membrane attack complex (MAC), which contains complement C5b, C6, C7, C8 and C9 proteins (C5b–9). Our previous studies have demonstrated that complement depletion or complement inhibition reduces brain injury in a rat ICH model [2, 3].

Activating microglia/macrophages enhances hematoma resolution and improves functional outcome in a rat ICH model [4, 5]. CD47, also called integrin-associated protein, is expressed on RBCs and other cells regulating target cell phagocytosis [6]. On normal RBCs, CD47 inhibits phagocytosis via interaction with an inhibitory receptor, signal regulatory protein alpha (SIRPα), on phagocytes. Our recent study showed that CD47 on RBCs has a role in clot removal following ICH[7].

Hematoma resolution is associated with the release of hemoglobin and hemoglobin-derived iron [1]. A hemoglobin scavenger receptor, CD163, on microglia/macrophages mediates the endocytosis of hemoglobin released from RBCs [8]. CD163 transports hemoglobin into microglia/macrophages with the subsequent induction of heme oxygenase-1 (HO-1) [8]. HO-1, a rate-limiting enzyme for heme degradation, is also considered as a modulator of erythrophagocytosis [9]. Deferoxamine (DFX), an iron chelator, reduces brain edema, white matter injury and neuronal cell death in rat and pig ICH models[10, 11], and it also reduces clot lysis after ICH[12].

The present study examined the process of hematoma clearance in a piglet ICH model. We also investigated the effect of DFX on clot lysis and erythrophagocytosis.

Materials and Methods

Animal preparation and intracerebral blood injection

Animal procedure protocols were approved by the University Committee on Use and Care of Animals, University of Michigan, and were conducted in accordance with United State Public Health Service's Policy on Humane Care and Use of Laboratory Animals. A total of 65 male piglets (8–10 kg; Michigan State University, East Lansing) were used in this study. One piglet was excluded because of high fever after surgery. The ICH models were performed as previously described [13, 14]. Pigs were sedated with ketamine (25 mg/kg, IM) and anesthetized with 2% isoflurane via nose cone. The isoflurane concentration was maintained at 1.0 to 1.5% during the surgical procedures. Core body temperature was maintained at 37.5 ± 0.5 °C by a feedback-controlled heating pad (Gaymar, Orchard Park, NY). The right femoral artery was inserted with a polyethylene catheter (PE-160) to obtain

blood for injection and to monitor arterial blood pressure, blood gases, and glucose concentrations. A cranial burr hole (1.5 mm) was drilled at the point 11 mm right of the sagittal suture and 11 mm anterior to the coronal suture. An 18-mm-long 20-gauge sterile plastic catheter was placed stereotaxically into the center of the right frontal cerebral white matter at the level of the caudate nucleus. First, 1.0 mL of autologous arterial blood was infused over 10 min with an infusion pump. Then 1.5 mL blood was injected over 10 min after a 5 min break. After injection, the needle was removed, the burr hole was filled with bone wax, and the skin incision was closed with sutures.

Experimental groups

There were two parts in this study. In the first part, piglets had ICH in the right frontal lobe. Brains were harvested at 4 hours or days 1, 3 and 7 (n=8 each group) for brain histology, ELISA and Western blots. In the second part, piglets had ICH in the frontal lobe and were treated with vehicle (saline) or deferoxamine (50 mg/kg, IM at 2 h after ICH and then every 12 h for up to 7 days). Brains were harvested at days 3 (n=8 each group) and 7 (n=8 each group) for brain histology, ELISA and Western blots.

Brain *in situ* freezing and brain histology

Brains were frozen in situ by decanting liquid nitrogen into a 12 oz. bottomless foam cup adhered to the head with Dow-Corning high vacuum grease (Dow Corning, Midland, MI), as described previously [15]. The duration time of this process usually took about 1 hour and the head was removed after the injection of potassium chloride to stop the heart beating. The frozen head was then cut with a band saw into 5 mm thick coronal sections. Tissues were sampled from the points of interest.

For brain histology, piglets were reanesthetized and the brains perfused in situ with 10% formalin. Brains were sectioned coronally. Paraffin embedded brain was cut into 10 μm thick sections.

Enzyme-linked immunosorbent assay (ELISA)

For hemoglobin and MAC measurement, the brains were *in situ* frozen and hematoma tissue samples were collected and homogenized[16]. The amount of hemoglobin and MAC were measured using Pig Hemoglobin Elisa kit (LifeSpan Biosciences, LS-F8543) and Pig C5b-9 Terminal Complement Complex Elisa kit (LifeSpan Biosciences, LS-F6300) respectively, according to the manufacturer's instructions.

Hematoxylin and eosin staining (H&E) and measurement of RBC diameter

H&E staining was used to examine RBC morphology and erythrocyte phagocytosis. Images were processed with Image J for measuring the diameter of RBC. The means were calculated from 30 RBCs per microscopic field in the hematoma edge and hematoma center, respectively, and 3 sections were analyzed for each brain.

Immunohistochemistry and cell counting

Immunohistochemistry staining was performed as described previously [14]. Briefly, the sections were deparaffinized in xylene and rehydrated in a graded series of alcohol dilutions.

Antigen retrieval was performed by the microwave method with citrate buffer (10 mM, pH 6.0). Immunohistochemistry studies were performed with avidin-biotin complex techniques. The primary antibodies were polyclonal rabbit anti-HO-1 (Enzo, ADI-SPA-895-F, 1:400 dilution) and CD163 (AbD, MAC342R, 1:100 dilution). Counting of CD163-positive cells was performed on high-power images (40× magnification) taken using a digital camera. Counts were performed on 4 areas in each brain section.

Western blotting

Western blot analysis was performed as previously described [14]. Briefly, brains were *in situ* frozen and the hematoma was sampled. Protein concentration was determined by Bio-Rad protein assay kit (Hercules, CA, USA). An equal amount of protein (50μg) was suspended in loading buffer, denatured at 95°C for 5 min, and loaded on an SDS-PAGE gel. After being electrophoresed and transferred onto Hybond-C pure nitrocellulose membrane (Amersham), the membrane was blocked with nonfat milk buffer for 2 h and then incubated with the primary antibodies. The primary antibodies were polyclonal rabbit anti-HO-1 (Enzo, ADI-SPA-895-F, 1:1000 dilution), monoclonal mouse anti-human CD47 (AbD, MCA911, 1:1000 dilution) and monoclonal mouse anti-GAPDH (Fitzgerald, 10R-G109A, 1:10000 dilution). The membranes were incubated with horseradish-peroxidase-conjugated secondary antibodies for 1 hour at room temperature. Protein band densities were detected by Kodak X-OMAT film and quantified by NIH Image J. HO-1 and CD47 levels in the hematoma were expressed as the ratio of HO-1/GAPDH or CD47/GAPDH.

Statistical analysis

Measurements were performed by personnel blinded to treatment groups. All the data are expressed as means ± SD. Data were analyzed by Student *t* tests or one-way analysis of variance (ANOVA). Differences were considered significant at $p<0.05$.

Results

The process of hematoma resolution was examined on coronal sections of pig brain after H&E staining. Erythrocyte lysis occurs in the hematoma. To examine whether the morphology of RBC changed in the development of hemorrhage resolution, the diameters of RBC in the hematoma edge and hematoma center were measured. We found that diameter of RBC decreased gradually in the hematoma edge and hematoma center (e.g. day-3 at hematoma edge: 2.71 ± 0.38μm vs. 3.89 ± 0.35μm at 4 hours, $p<0.01$; hematoma center: 2.61 ± 0.29 μm vs. 3.75 ± 0.25μm at 4 hours, $p<0.01$. Fig. 1). The majority of RBCs at 4 hour after ICH were of double-faced concave disc shape (“discocyte”; Fig. 1). RBCs in hematoma edge were fairly irregular in shape with spike at day-3 after ICH, whereas the RBC in center-hematoma deformed into uniformly sized spherical cells (“spherocyte”; Fig. 1). The transformation of erythrocyte shape from discocyte to spherocyte might be due to changes in membrane permeability.

Hemoglobin contents in the clot (Fig. 2A) were measured to assess hematoma resolution. The level of hemoglobin declined gradually over the time after the onset of ICH with a

significant reduction at day 3. The contents of hemoglobin in the clot were 26.2 ± 5.2 mg/g at 4 hours, but were reduced to 13.9 ± 0.9 mg/g at day-3 (Fig. 2B, $p<0.01$).

Activation of the complement system and the formation of MAC resulted in an increased membrane permeability and erythrocyte lysis. In this present study, MAC contents in the clot gradually increased with a marked accumulation at day-3 (53.5 ± 8.2 vs. 11.0 ± 3.9 ng/g at 4 hour, $p<0.01$, Fig. 2C) and stayed at high levels at day 7.

Erythrophagocytosis was observed in the hematoma edge at day-3 (Fig. 3A), and hemosiderin deposition was identifiable in the hematoma edge at day-7 (Fig. 3A). RBCs in the hematoma center started to be phagocytized by macrophages/microglia at day-7 (Fig. 3A). The expression of CD 47 in hematoma was high during the first day after ICH and was significantly reduced at day-3 ($p<0.01$ vs. 4 hours and $p<0.05$ vs. day-1, Fig. 3B). It remained at low levels at day-7 (Fig. 3B).

CD163 and HO-1 positive cells infiltrated into the hematoma from edge to center after ICH (Figs. 4A & 4B). A significant increase of CD163 cells was found at day 3. HO-1 protein levels in the hematoma also increased at day-3 (HO-1/GAPDH: 0.65 ± 0.08 at day-3 vs. 0.04 ± 0.01 at 4 hour, $p<0.01$). The morphological characteristics of the CD 163 and HO-1 positive cells in the clot were microglia/macrophage-like.

To investigate whether DFX affects the process of hematoma resolution, the ICH piglets were treated with DFX or vehicle for 3 days. We found that hemoglobin contents in hematoma were significantly higher in the DFX treated group compare to the vehicle-treated group (15.9 ± 1.8 vs. 11.8 ± 0.8 mg/g, $p<0.05$, Fig. 5A). DFX also reduced the MAC content in the clot at day-3 (33.0 ± 6.6 vs. 56.2 ± 9.2 ng/g in the vehicle-treated group, $p<0.05$, Fig. 5B). These results suggested that the treatment of DFX reduced the process of hemolysis after ICH, which might be due to alleviating MAC formation.

Whether DFX had an effect on CD 47 and erythrophagocytosis in the clot was also examined. The loss of CD47 in the clot was reduced significantly by DFX treatment at day 3 (CD47/GAPDH: 1.32 ± 0.16 in ICH+DFX group vs. 0.74 ± 0.07 in ICH + vehicle group, $p<0.05$, Fig. 5C) and day 7 ($p<0.01$, Suppl Figure I). DFX treatment also caused a significant reduction in infiltrating CD163-positive and HO-1 positive cell in the hematoma at day 3 (Figs. 6A and B) and day 7 (Suppl Figures II & III). Western blot analysis showed that the protein expression of HO-1 was decreased in the hematoma in the DFX treated group at day 3(HO-1/GAPDH: 0.32 ± 0.04 vs. 0.98 ± 0.07 in the vehicle-treated group, $p<0.05$, Fig. 6B) and day 7 ($p<0.05$, Suppl Figure III).

Discussion

The major findings of this study are: 1) RBCs in the clot become smaller with time; 2) a gradual increase in clot MAC levels with a progressive decrease in hemoglobin levels; 3) a steady decrease in clot CD47 levels with time which may be linked to significant erythrophagocytosis; 4) increases in the number of CD 163- and HO-1 positive cells infiltrating into the hematoma with time; 5) DFX attenuated MAC formation and erythrophagocytosis.

The diameter of RBCs within the hematoma decreased with time after ICH. This may be linked to complement-mediated cell lysis. The present study demonstrates that MAC accumulation in the clot with time. RBCs are sensitive to complement-dependent hemolysis with MAC formation. Following complement cascade activation, MAC on the cell membrane forms a pore resulting in membrane permeability changes[17] finally leading to RBC morphological alterations and erythrocyte lysis. The cell membrane abnormalities induce a morphological change in RBC from discocyte to spherocyte with a gradual decrease in RBC diameter [18, 19]. It should be noted, however, that other factors may cause a reduction in RBC size. For example, shrinkage occurs in RBCs undergoing eryptosis, a form of suicidal cell death in erythrocytes [20]. Whether eryptosis occurs in the hematoma needs further study.

Phagocytosis of erythrocytes by microglia/macrophages has a role in hematoma clearance after ICH [7]. The current study examined the natural time course of CD47 expression in the hematoma in a swine ICH model and found that CD47 levels in the clot decrease with time. We also showed that reduction of CD47 levels in the clot is associated with microglia/macrophage infiltration. CD47, as a “don’t eat me” signal, is expressed on RBCs, and has an important role in regulating erythrophagocytosis [7]. CD47 exerts its inhibitory effect on phagocytosis through binding to inhibitory immunoreceptor SIRPα expressed by microglia/macrophages [21]. Thus, the CD47-SIRPα constitutes a negative feedback for erythrophagocytosis[22]. The loss of CD47 expression in RBCs may initiate erythrophagocytosis after ICH, and lead to hematoma clearance. Our recent study showed that depleting CD47 in RBCs resulted in faster hematoma clearance with microglia/macrophages being less likely to phagocytize RBCs with CD47 than CD47-deficient RBC [7]. However, it should also be noted that perihematomal brain CD47 levels were increased in this pig model of ICH[13]. The precise role of CD47 in brain cells needs to be studied further.

Microglia are brain-resident phagocytic cells that are activated in response to injury stimuli. The transformation of inactive microglia into phagocytic phenotype is associated with alterations in cell surface receptors[23]. Evidence suggested that CD163 acts as a hemoglobin scavenger receptor on microglia/macrophage with a role in erythrophagocytosis [8]. With more studies on microglia/microphage polarization, CD163 is classified into the marker of alternatively activated phenotype (M2 phenotype, phagocytic phenotype) [23–25]. CD163 mediated hemoglobin/hematoma clearance is involved in the induction of HO-1, a rate-limiting enzyme for heme degradation [26]. Usually HO-1 is considered as an oxidative stress protein in microglia and related to brain injury after ICH[11]. A recent study, however, indicated that HO-1 is associated with blood clearance by enhancing erythrophagocytosis after stroke [9]. In the current study, we found that the infiltration of CD163 and HO-1 positive cells into the hematoma increased with time paralleling hematoma resolution. Whether HO-1 is involved in regulating erythrophagocytosis after ICH should be tested further.

Our studies have showed that DFX has a neuroprotective effect on brain injury after ICH, mainly due to iron detoxification[10, 27]. The present study found that DFX treatment reduces MAC formation in the clot. Less MAC accumulation in the clot may result in reduced RBC lysis and less brain iron overload. DFX also reduced CD47 loss and microglia/macrophage

infiltration after ICH suggesting it also affects erythrophagocytosis. In combination, these finding may underlie our previous results showing that DFX slows hematoma resolution after ICH in aged rats [12]. Our future studies will test effects of a combination therapy (iron chelation plus erythrophagocytosis enhancement) on ICH-induced brain injury.

Although this is a novel study focusing on changes in the hematoma using a large animal model of ICH, there are several limitations: 1) hematoma sizes were not measured; 2) a causal relationship MAC accumulation and hematoma clearance was not established; and 3) it is still unclear whether hemolysis or phagocytosis is the main process of clot clearance.

In summary, this study presents data on the natural history of hematoma resolution after ICH in a piglet model. Hemolysis and erythrophagocytosis are associated with hematoma resolution following ICH, which is modified by DFX. This study provides important information regarding hematoma resolution and informs future studies on how to manipulate that process.

Supplementary Material

Refer to Web version on PubMed Central for supplementary material.

Acknowledgments

Sources of Funding: This study was supported by grants NS-084049, NS-091545, NS-090925, NS-073595, and NS-079157 from the National Institutes of Health (NIH).

References

1. Xi G, Keep RF, Hoff JT. Mechanisms of brain injury after intracerebral hemorrhage. Lancet Neurol. 2006; 5:53–63. [PubMed: 16361023]
2. Hua Y, Xi G, Keep RF, Hoff JT. Complement activation in the brain after experimental intracerebral hemorrhage. J Neurosurg. 2000; 92:1016–1022. [PubMed: 10839264]
3. Xi G, Hua Y, Keep RF, Younger JG, Hoff JT. Systemic complement depletion diminishes perihematomal brain edema in rats. Stroke. 2001; 32:162–167. [PubMed: 11136932]
4. Zhao X, Grotta J, Gonzales N, Aronowski J. Hematoma resolution as a therapeutic target: The role of microglia/macrophages. Stroke. 2009; 40:S92–94. [PubMed: 19064796]
5. Zhao X, Sun G, Zhang J, Strong R, Song W, Gonzales N, et al. Hematoma resolution as a target for intracerebral hemorrhage treatment: Role for peroxisome proliferator-activated receptor gamma in microglia/macrophages. Ann Neurol. 2007; 61:352–362. [PubMed: 17457822]
6. Oldenborg PA, Zheleznyak A, Fang YF, Lagenaur CF, Gresham HD, Lindberg FP. Role of cd47 as a marker of self on red blood cells. Science. 2000; 288:2051–2054. [PubMed: 10856220]
7. Ni W, Mao S, Xi G, Keep RF, Hua Y. Role of erythrocyte cd47 in intracerebral hematoma clearance. Stroke. 2016; 47:505–511. [PubMed: 26732568]
8. Abraham NG, Drummond G. Cd163-mediated hemoglobin-heme uptake activates macrophage ho-1, providing an antiinflammatory function. Circ Res. 2006; 99:911–914. [PubMed: 17068296]
9. Schallner N, Pandit R, LeBlanc R 3rd, Thomas AJ, Ogilvy CS, Zuckerbraun BS, et al. Microglia regulate blood clearance in subarachnoid hemorrhage by heme oxygenase-1. J Clin Invest. 2015; 125:2609–2625. [PubMed: 26011640]
10. Keep RF, Hua Y, Xi G. Intracerebral haemorrhage: Mechanisms of injury and therapeutic targets. Lancet Neurology. 2012; 11:720–731. [PubMed: 22698888]
11. Xi G, Strahle J, Hua Y, Keep RF. Progress in translational research on intracerebral hemorrhage: Is there an end in sight? Prog Neurobiol. 2014; 115C:45–63.

12. Hatakeyama T, Okauchi M, Hua Y, Keep RF, Xi G. Deferoxamine reduces neuronal death and hematoma lysis after intracerebral hemorrhage in aged rats. Transl Stroke Res. 2013; 4:546–553. [PubMed: 24187595]
13. Zhou X, Xie Q, Xi G, Keep RF, Hua Y. Brain cd47 expression in a swine model of intracerebral hemorrhage. Brain Res. 2014; 1574:70–76. [PubMed: 24931767]
14. Xie Q, Gu Y, Hua Y, Liu W, Keep RF, Xi G. Deferoxamine attenuates white matter injury in a piglet intracerebral hemorrhage model. Stroke. 2014; 45:290–292. [PubMed: 24172580]
15. Wagner KR, Xi G, Hua Y, Kleinholz M, de Courten-Myers GM, Myers RE. Early metabolic alterations in edematous perihematomal brain regions following experimental intracerebral hemorrhage. J Neurosurg. 1998; 88:1058–1065. [PubMed: 9609301]
16. Wagner KR, Xi G, Hua Y, Kleinholz M, de Courten-Myers GM, Myers RE, et al. Lobar intracerebral hemorrhage model in pigs: Rapid edema development in perihematomal white matter. Stroke. 1996; 27:490–497. [PubMed: 8610319]
17. Nicholson-Weller A, Halperin JA. Membrane signaling by complement c5b-9, the membrane attack complex. Immunol Res. 1993; 12:244–257. [PubMed: 8288945]
18. Motoyama K, Arima H, Toyodome H, Irie T, Hirayama F, Uekama K. Effect of 2,6-di-o-methyl-alpha-cyclodextrin on hemolysis and morphological change in rabbit's red blood cells. Eur J Pharm Sci. 2006; 29:111–119. [PubMed: 16870405]
19. Blasi B, D'Alessandro A, Ramundo N, Zolla L. Red blood cell storage and cell morphology. Transfus Med. 2012; 22:90–96. [PubMed: 22394111]
20. Lang F, Qadri SM. Mechanisms and significance of eryptosis, the suicidal death of erythrocytes. Blood purification. 2012; 33:125–130. [PubMed: 22269222]
21. Burger P, Hilarius-Stokman P, de Korte D, van den Berg TK, van Bruggen R. Cd47 functions as a molecular switch for erythrocyte phagocytosis. Blood. 2012; 119:5512–5521. [PubMed: 22427202]
22. Olsson M, Nilsson A, Oldenborg PA. Target cell cd47 regulates macrophage activation and erythrophagocytosis. Transfus Clin Biol. 2006; 13:39–43. [PubMed: 16564725]
23. Franco R, Fernandez-Suarez D. Alternatively activated microglia and macrophages in the central nervous system. Prog Neurobiol. 2015; 131:65–86. [PubMed: 26067058]
24. Durafourt BA, Moore CS, Zammit DA, Johnson TA, Zaguia F, Guiot MC, et al. Comparison of polarization properties of human adult microglia and blood-derived macrophages. Glia. 2012; 60:717–727. [PubMed: 22290798]
25. David S, Kroner A. Repertoire of microglial and macrophage responses after spinal cord injury. Nat Rev Neurosci. 2011; 12:388–399. [PubMed: 21673720]
26. Herz J, Strickland DK. Lrp: A multifunctional scavenger and signaling receptor. J Clin Invest. 2001; 108:779–784. [PubMed: 11560943]
27. Gu Y, Hua Y, Keep RF, Morgenstern LB, Xi G. Deferoxamine reduces intracerebral hematoma-induced iron accumulation and neuronal death in piglets. Stroke. 2009; 40:2241–2243. [PubMed: 19372448]

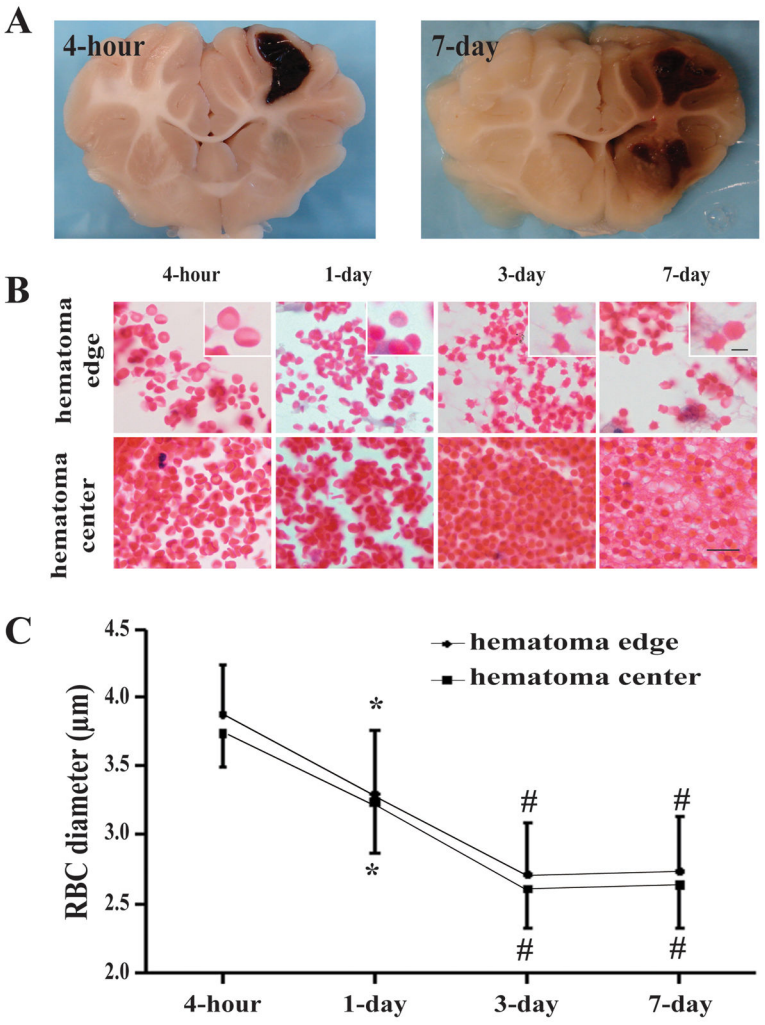

Figure 1.

(A) Coronal sections of perfused piglet brain showing hematomas. (B) Time course of clot changes in hematoma edge and center. Scale bar = 10 μm, scale bar = 2.5 μm in the insets. (C) Diameter of RBC in hematoma edge and center. Values are mean ± SD, *p <0.05, #p <0.01 vs. 4-hour.

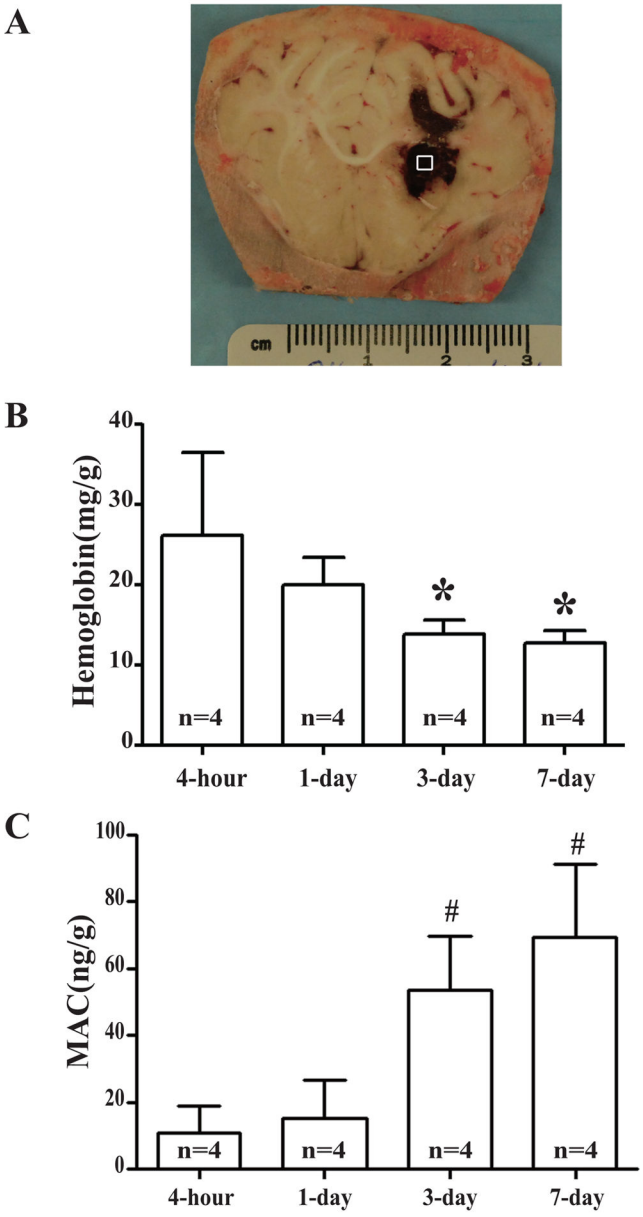

Figure 2.

(A) Coronal section of an *in situ* frozen piglet brain after ICH. The square represents the sample area. (B) Time course of hemoglobin content in hematoma. Values are mean ± SD, *p <0.05, #p <0.01 vs. 4-hour. (C) Time course of MAC content in the hematoma. Values are mean ± SD, *p <0.05, #p <0.01 vs. 4-hour.

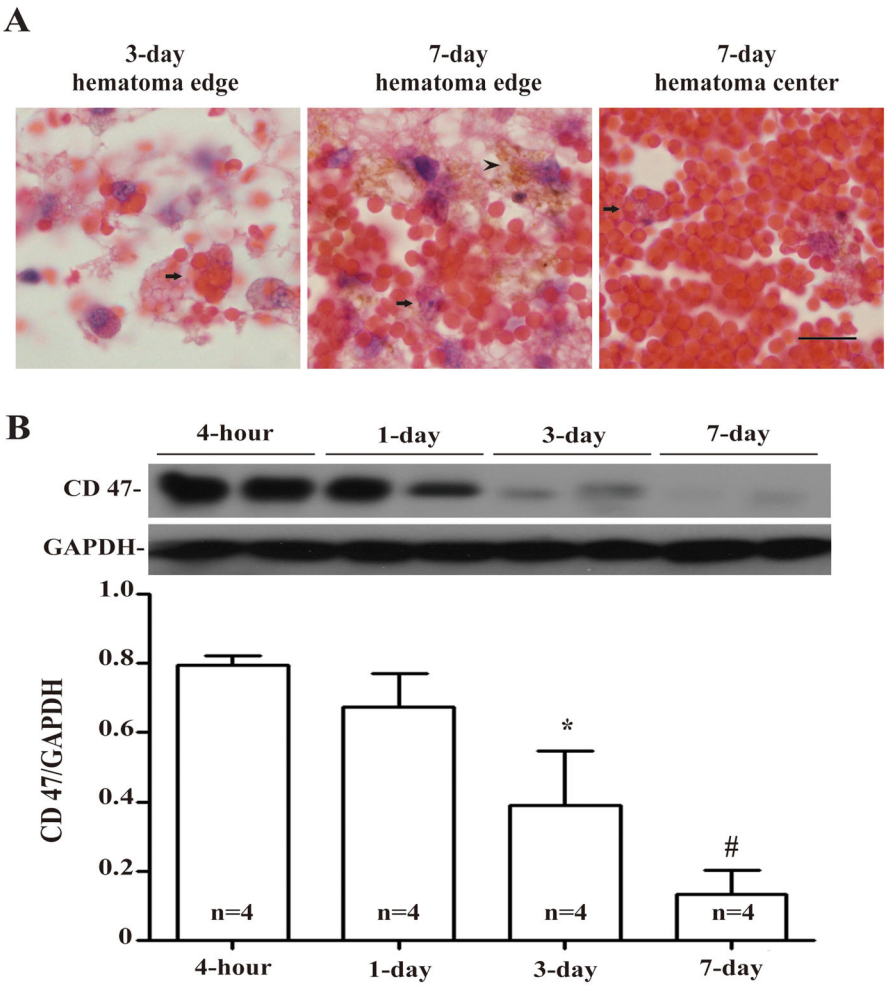

Figure 3.

(A) Erythrophagocytosis (arrows) at day-3 and day-7 in the hematoma and hemosiderin deposition (arrowhead) at day-7. Scale bar = 10 μm. (B) Time course of CD47 levels in the hematoma. Values are mean ± SD, *p <0.05, #p <0.01 vs. 4-hour.

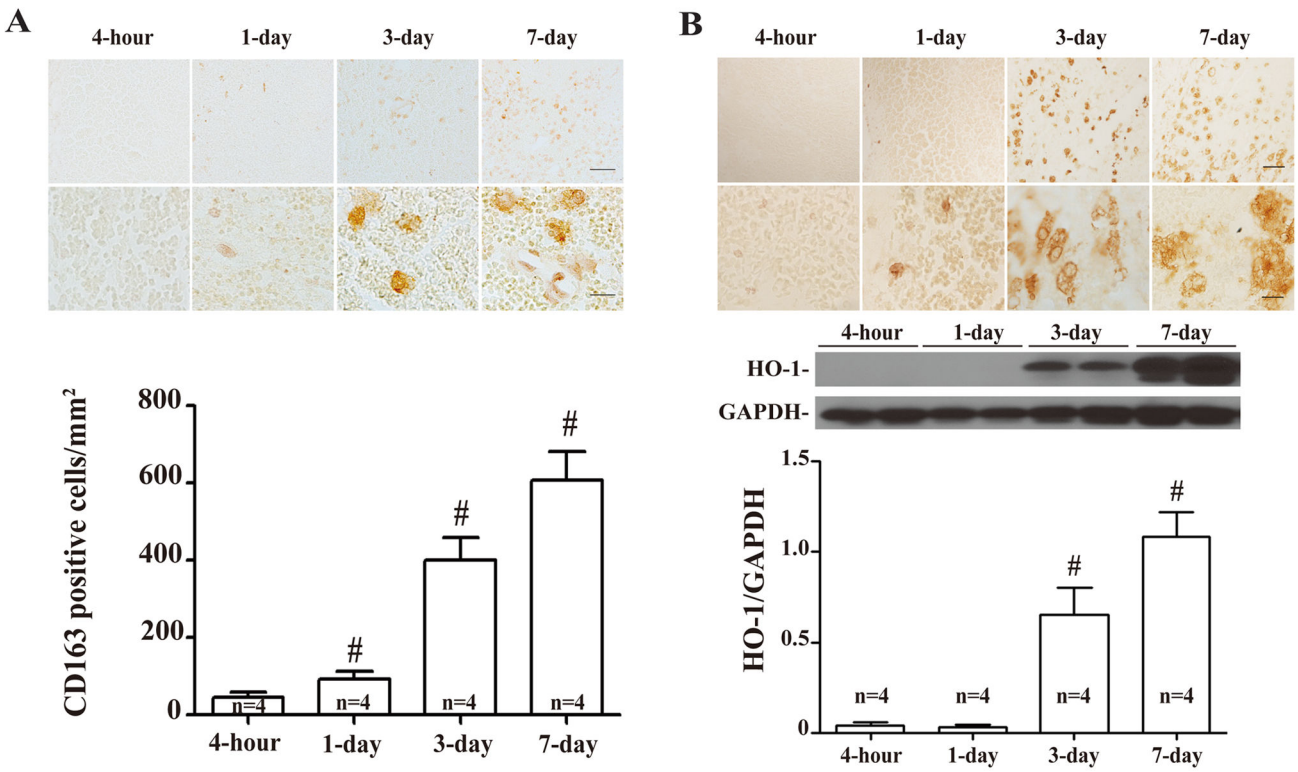

Figure 4.

(A) Time course of CD163 immunoreactivity and number of positive cells in the hematoma. Upper scale bar = 50μm, lower scale bar = 10μm. Values are mean ± SD, **p* <0.05, #*p* <0.01 vs. 4-hour. (B) Time course of HO-1 immunoreactivity and protein levels. Upper scale bar = 50 μm, lower scale bar = 10 μm. Values are mean ± SD, **p* <0.05, #*p* <0.01 vs. 4-hour.

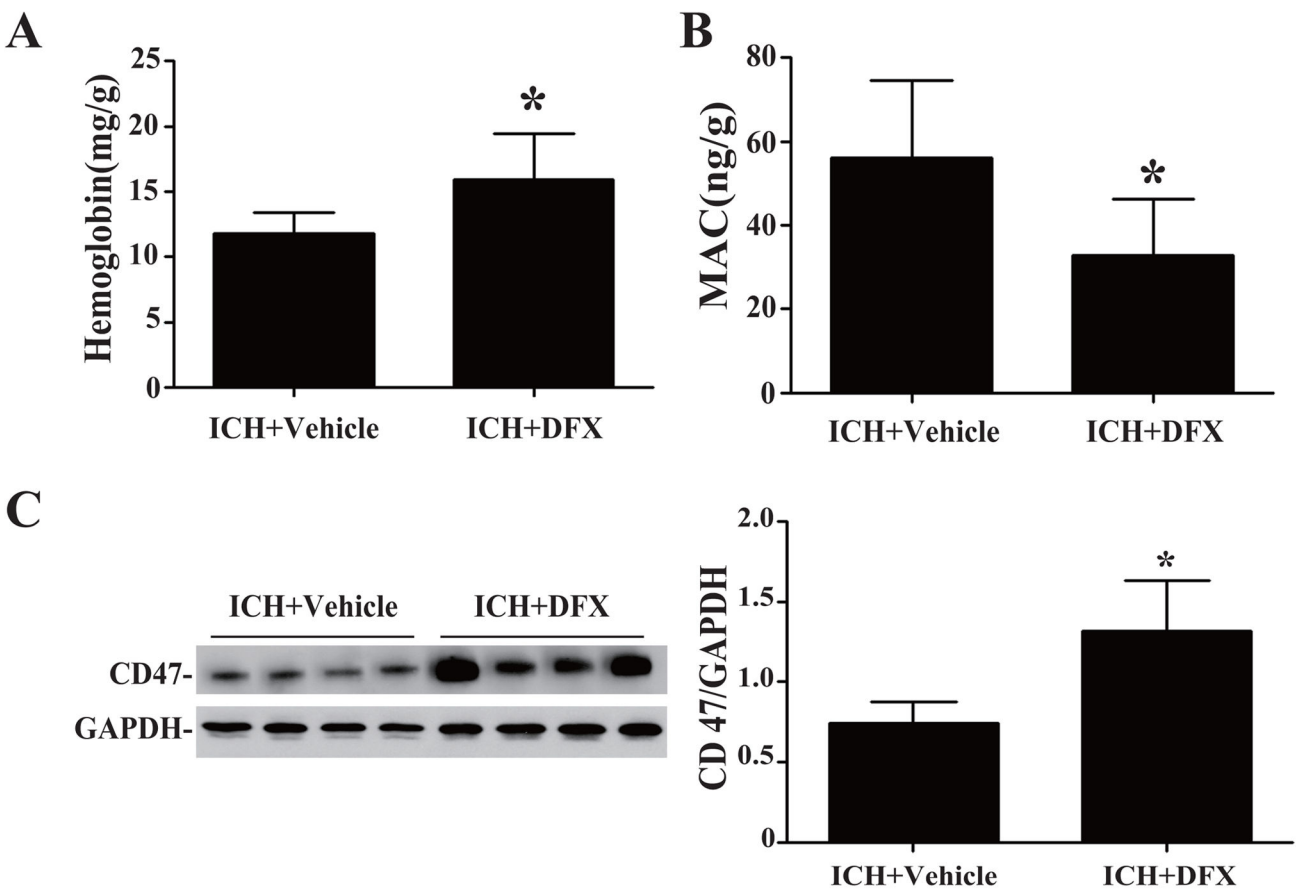

Figure 5.

(A) Hemoglobin, (B) MAC and (C) CD47 protein levels in the hematoma in vehicle- and DFX-treated groups at 3 days after ICH. Values are mean ± SD, *p <0.05 vs. vehicle treated group.

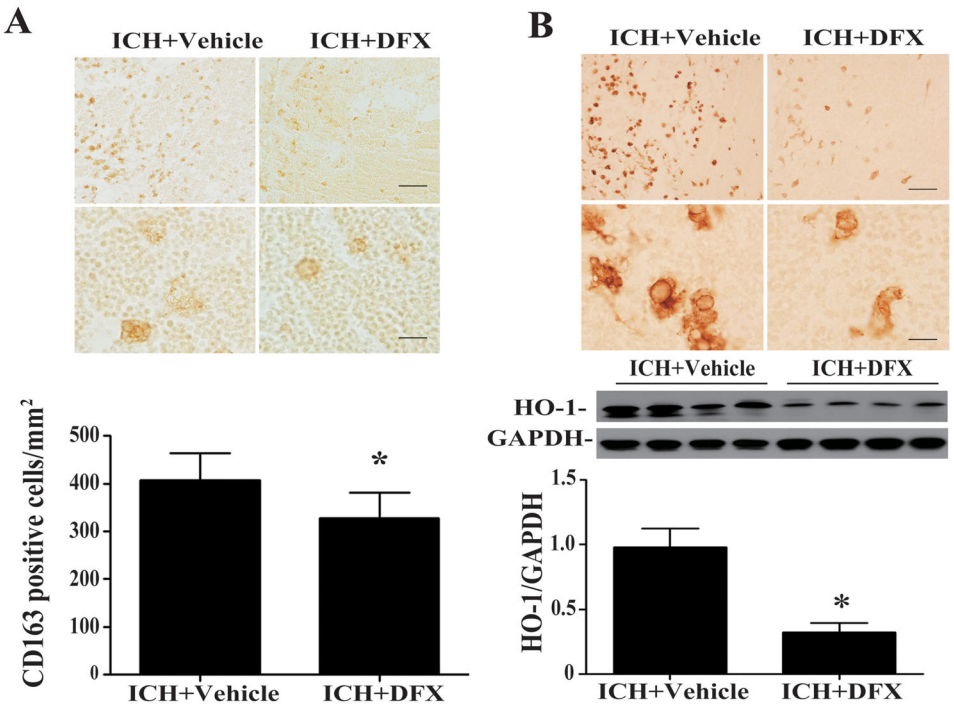

Figure 6.

(A) CD163 immunoreactivity and numbers of positive cells in the hematoma in vehicle- and DFX-treated groups at 3 days after ICH. Upper scale bar = 50 μm, lower scale bar = 10 μm. Values are mean ± SD, *p <0.05. (B) HO-1 immunoreactivity and proteins levels in the hematoma in vehicle- and DFX-treated groups at 3 days after ICH. Upper scale bar = 50 μm, lower scale bar =10 μm. Values are mean ± SD, *p <0.05.